



Published in final edited form as:

*J Mater Chem B Mater Biol Med.* 2017 July 28; 5(28): 5580–5587. doi:10.1039/C7TB00974G.

## A General Strategy for Generating Gradients of Bioactive Proteins on Electrospun Nanofiber Mats by Masking with Bovine Serum Albumin

Michael L. Tanes<sup>a</sup>, Jiajia Xue<sup>a</sup>, and Younan Xia<sup>a,b</sup>

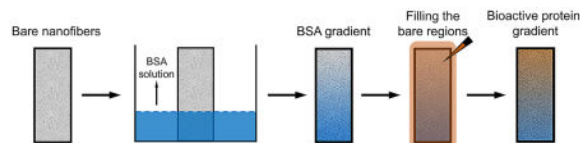
<sup>a</sup>The Wallace H. Coulter Department of Biomedical Engineering, Georgia Institute of Technology and Emory University, Atlanta, Georgia 30332, United States

<sup>b</sup>School of Chemistry and Biochemistry, School of Chemical and Biomolecular Engineering, Georgia Institute of Technology, Atlanta, Georgia 30332, United States

### Abstract

Electrospun nanofibers are widely used in tissue engineering owing to their capability to mimic the structures and architectures of various types of extracellular matrices. However, it has been difficult to incorporate a biochemical cue into the physical cue provided by the nanofibers. Here we report a simple and versatile method for generating gradients of bioactive proteins on nanofiber mats. We establish that the adsorption of bovine serum albumin (BSA) onto nanofibers is a time- and concentration-dependent process. By linearly increasing the volume of BSA solution introduced into a container, a gradient in BSA is readily generated across the length of a vertically oriented strip of nanofibers. Next, the bare regions uncovered by BSA can be filled with the bioactive protein of interest. In demonstrating the potential application, we examine the outgrowth of neurites from dorsal root ganglion (DRG) isolated from chick embryos and then seeded on aligned polycaprolactone nanofibers covered by nerve growth factor (NGF) with a uniform coverage or in a gradient. In the case of uniform coverage, the neurites extending from DRG show essentially the same length on either side of the DRG cell mass. For the sample with a gradient in NGF, the neurites extending along the gradient (*i.e.*, increase of NGF concentration) were significantly longer than the neurites extending against the gradient.

### Graphical abstract



### Keywords

Electrospun nanofiber; Protein gradient; Chemotaxis; Neural tissue engineering

## 1. Introduction

Protein gradients play key roles in the development and growth of human bodies, and healing of wounds, as well as generation and progression of diseases. Specifically, protein gradients can encourage and direct the growth of peripheral nerves in the developing fetus,<sup>1,2</sup> attract and guide immune cells to the sites of injury or infection,<sup>3,4</sup> and recruit blood vessels into hypoxic tumors.<sup>4</sup> In the area of regenerative medicine, protein gradients have become a powerful means for the enhancement of tissue regeneration by directing and influencing the migration, extension, and differentiation of cells.<sup>5-7</sup> To this end, people have manipulated the release and diffusion of proteins (or other bio-effectors) from point sources or across microfluidic channels to induce the formation of protein gradients.<sup>1,2,8-12</sup> In general, the gradients derived from point sources can only last until the encapsulated species are depleted while the microfluidic devices are confined to a limited set of substrates or configurations. Another strategy, which produces persistent gradients and shows great versatility, is based on patterning the surface of gel substrates, made of polydimethylsiloxane or poly(ethylene glycol), with proteins.<sup>9,13</sup> Although gels can mimic the disorganized soft-tissue environment, many of the tissues in the body contain a highly organized extracellular matrix (ECM), such as tendon,<sup>14</sup> muscle,<sup>15</sup> nerve tissue,<sup>16</sup> and blood vessels.<sup>17</sup> In these cases, integrating a persistent gradient of proteins with a polymer scaffold made of aligned fibers could significantly improve the outcome of tissue regeneration by accelerating cell proliferation and migration.

Electrospun nanofibers can be employed to mimic the structures and functions of collagen fibers found in the native ECM. In particular, electrospun nanofibers can be aligned and stacked to recapitulate the structural organization of ECMs in various types of tissues.<sup>18</sup> One of the major challenges in using nanofibers as scaffolds for tissue engineering is the incorporation of biochemical cues. Strategies that have been reported in literatures range from encapsulation to electrostatic attraction, adsorption, and covalent immobilization.<sup>19-25</sup> The next step is to adapt these strategies for producing gradients on nanofibers and a review of the literature reveals a number of attempts. For example, Kim *et al.* created a gradient of physical properties, such as hydrophobicity, through the thickness of a nanofiber mat, but did not incorporate gradients of biochemical cues.<sup>26</sup> As a rudimentary step to control the extent of a peptide exposed on the surface of a nanofiber, Viswanathan *et al.* formulated their electrospinning solution by blending two different block co-polymers at varying ratios.<sup>27</sup> Even if this strategy were adapted to produce a spatial gradient of a peptide or protein in the future, the use of exotic block co-polymers greatly limits the scope of application. Dinis *et al.* created a gradient of encapsulated nerve growth factor (NGF) by electrospinning uniaxially aligned nanofibers with a large amount of proteins and then cutting away all but a small portion of the fibers. They repeated the process while successively reducing the amount of encapsulated NGF and the portion of fibers cut away until a full gradient was formed.<sup>28</sup> While this strategy allows for a control over the gradient profile and composition, the gradient is ultimately discrete and the changes in protein concentration would appear as large steps at the length scale of a mammalian cell. To fabricate a gradient of covalently immobilized drug or peptide on the surface of extruded polymer nanofibers, Kim *et al.* exposed pre-deposited benzophenone to UV light under a gradient photomask and then

immobilized the biochemical cue *via* a click-chemistry reaction.<sup>29</sup> This particular strategy allows for an unprecedented control over the gradient profile and can incorporate as many different protein gradients as there are orthogonal click-chemistry reactions. As a major drawback, this strategy requires the use of specially functionalized benzophenone compounds and proteins. A much simpler approach to the creation of a gradient is based on the notion of varying the immersion time of a nanofiber mat in a solution along one axis. This approach has been successfully applied to generate gradients of fibronectin, mineral content, and even cells.<sup>30-33</sup> To summarize, some of the major disadvantages with the current methods for generating gradients on nanofibers include the requirement of overly complicated protocols, involvement of exotic materials, and use of a relatively large amount and thus waste of the bioactive protein.

Here we report a general strategy for generating gradients of bioactive proteins on mats of electrospun nanofibers. Figure 1 shows a schematic illustration of the two major steps involved. Specifically, bovine serum albumin (BSA) is deposited on the surface of nanofibers in a gradient to serve as a mask for the deposition of a bioactive protein of interest. The bioactive protein fills into the bare regions left behind on the surface to generate a gradient that runs countercurrent to the BSA gradient. By creating a BSA mask instead of depositing the bioactive protein directly, the limited and expensive bioactive protein can be saved by not wasting them in the considerable volume of solution typically needed to generate the gradient. Instead, the relatively inexpensive and abundant BSA is exploited. Additionally, the conditions required to produce the gradient only need be optimized once for BSA, rather than being scrutinized again and again for different types of bioactive proteins. As a proof-of-concept demonstration for potential application in tissue engineering, we functionalize the surface of uniaxially aligned nanofibers with NGF as a uniform coating and in a gradient and then culture embryonic chick dorsal root ganglion (DRG) on top of the nanofibers to examine the outgrowth of neurites. Our results clearly show the influence of NGF gradient on the extension of neurites, in addition to the physical cue provided by the aligned nanofibers.

## 2. Materials & Methods

### 2.1 Materials

BSA, BSA labeled with fluorescein (BSA-FITC), polycaprolactone (PCL, 80,000 g/mol in average molecular weight), formaldehyde, pyridine, formic acid, dimethylformamide (DMF), dichloromethane (DCM), phosphate-buffered saline (PBS), Tween 20, and anti-neurofilament 200 were all purchased from Sigma-Aldrich (St. Louis, MO). Pyridine and formic acid were mixed in equimolar amounts to produce pyridinium formate (PF).<sup>34</sup> Silastic Type A Medical Adhesive was purchased from Dow Corning (Midland, MI). Hank's buffered salt solution (HBSS), neural basal media, N-2 supplement, antibiotic antimycotic (ABAM), and Alexa Fluor 488 goat anti-mouse IgG were all purchased from Invitrogen (Carlsbad, CA). NGF was obtained from R&D system (Minneapolis, MN).

## 2.2 Electrospinning of PCL Nanofibers

Pellets of PCL were dissolved at a concentration of 5% w/v in a mixed solution composed of PF, DMF, and DCM at a volume ratio of 5:15:80 and sonicated in cold water for about 1 h. The PCL solution was then pumped out from a syringe at a rate of 0.5 mL/h using a syringe pump (KD Scientific, Holliston, MA). Aluminum foil, as the grounded collector, was placed 20 cm away from the needle tip and a voltage of 18 kV was applied between them (Gamma High Voltage Research, Ormond Beach, FL). The ambient atmospheric conditions were about 20 °C and 40% humidity. Electrospinning was terminated after 2.0 mL of PCL solution had been dispensed. To produce aligned nanofibers, a U-shaped steel collector was applied and the nanofibers were collected for 10 min.

## 2.3 Characterization of the Nanofibers

The morphology of electrospinning nanofibers was characterized by using scanning electron microscopy (SEM). The images were obtained for nanofiber sections that had been subjected to varying oxygen plasma (O<sub>2</sub>-plasma) exposure durations (0, 0.5, 1, 2, or 5 min) or had been separately soaked in a solution of PBS, 0.1% BSA, or 0.5% BSA for 1 h after O<sub>2</sub>-plasma-treatment for 2 min. Afterwards, the samples were coated with a Hummer 6 Au/Pd sputter (Anatech, Union City, CA) and imaged under a Hitachi 8230 cold field emission scanning electron microscope (Tokyo, Japan). The diameters of 100 nanofibers from each sample were evaluated by ImageJ software. Statistical significance was evaluated using Student's t-test. The static water contact angle of the nanofiber mat before and after O<sub>2</sub>-plasma-treatment for 2 min was separately measured using a SL200A type Contact Angle Analyzer at ambient temperature. A water droplet of 3.0 μL in volume was carefully placed on the surface of the nanofiber mat. The average water contact angle value was obtained by measuring ten water droplets at randomly distributed positions.

## 2.4 BSA Adsorption on PCL Nanofibers

Circular sections of 1 cm in diameter were punched out from a non-woven mat of PCL nanofibers, weighed, placed in 24-well plates, and exposed to O<sub>2</sub>-plasma for 2 min (PlasmaEtch, Carson City, NV). Afterwards, 1 mL of BSA solution at a concentration of 0.1% or 0.5% w/v was added into the wells with samples. After different periods of time, 5, 10, 20, 30, 45, and 60 min, respectively, the BSA solutions were removed and the nanofiber sections were rinsed with PBS three times to remove the free BSA. All time points were repeated in triplicate. Then, 70 μL of 0.5% w/v BSA-FITC in PBS solution was placed on each nanofiber section and kept in the dark at room temperature for 2 h. The sections were washed with 0.1% v/v Tween 20 in deionized H<sub>2</sub>O three times, rinsed with PBS three times, and then imaged using a Leica 6000 B inverted microscope (Buffalo Grove, IL).

The average fluorescent intensity of each nanofiber section was analyzed using MATLAB from the fluorescence micrographs and then normalized to the weight of the respective nanofiber section. After subtracting the initial normalized fluorescence value ( $c_0$ ,  $t=0$  min) from the respective 0.1% and 0.5% BSA sets, the fluorescence data were linearized using a Hanes-Woolf transform. By inverting the change in fluorescent intensity, multiplying by the time elapsed, and plotting against the time elapsed, the maximum BSA coverage ( $c_{max}$ ,

maximum normalized fluorescence) and time to half of maximum coverage ( $T_m$ ) values were obtained, as well as the function in the form of  $c(t) = c_0 - \frac{c_{\max} t}{T_m - t}$  for fitting the data.

## 2.5 Generation of Protein Gradients

Strips of nanofibers with a dimension of 40 mm long and 5 mm wide were cut out and mounted on glass slides with Silastic Type A Medical Adhesive. The starting and ending points with a 35 mm distance from each other were marked. After exposing to  $O_2$ -plasma for 2 min, the nanofiber strip was placed vertically in an empty beaker, and 0.1% BSA solution in PBS was added until the solution level reached the starting point. Then, the BSA solution was introduced at a rate of 3.0 mL/h using a pump. After the solution level reached the ending point, in about 1 h, the strip was removed from the BSA solution and immediately rinsed with PBS three times.

In order to visualize the resultant gradients after filling in the bare regions left behind by the BSA, 200  $\mu$ L of 0.5% BSA-FITC solution in PBS was pipetted onto each nanofiber strip and incubated in the dark at room temperature for about 2 h. Afterwards, the nanofiber strips were washed with 0.1% Tween 20 solution three times, rinsed with PBS three times, and covered with glass coverslips. The strips were imaged at three spots every 5 mm from the ending point (0 mm) to the starting point (35 mm) at 20x magnification. The average fluorescence intensity at each position was calculated using MATLAB and plotted. With the same procedure, we also produced gradient of BSA-FITC on the surface of pristine nanofiber strip by directly depositing 0.1% BSA-FITC solution onto a strip of nanofiber mat to observe the formation of BSA gradient in a more visual way. The strip was then imaged using an optical fluorescence microscope and the fluorescence intensities at different positions were calculated.

To produce a gradient of NGF on nanofibers for the neurite extension study, aligned PCL nanofibers were affixed to glass coverslips (22  $\times$  22 mm) and  $O_2$ -plasma-treated for 2 min. Two coverslips (oriented such that the fiber orientation ran vertically) were separately stood up in the wells of a 6-well plate, and then 0.1% BSA solution was pumped in over 1 h with a syringe pump. As controls, two sets of samples were immersed completely in 0.1% BSA solution or PBS for 1 h. Afterwards, all samples were rinsed in PBS three times and sterilized under UV light for 1 h. NGF (200  $\mu$ L of 10  $\mu$ g/mL solution) was pipetted onto the nanofibers with a BSA gradient or that had been immersed in PBS. As a control, PBS was placed on the nanofibers that had been completely immersed in BSA. All samples were then incubated at 4  $^{\circ}$ C overnight followed by rinsing with PBS three times and seeding DRG on.

## 2.6 Isolation and Culture of DRG

All DRG were isolated from the thoracic region of the spinal column in embryonic chicks *via* sterile microdissection. Embryonic day 8 (E8, stage HH35-36) chicks were removed from the white leghorn eggs and decapitated. DRG were dissected from the thoracic region and collected in HBSS. The DRG cells were then seeded onto the center of the samples (1 DRG per sample) and subsequently cultured for 6 days in a modified neurobasal medium

supplemented with 1% N-2 supplement and 1% ABAM, in the presence or absence of 50 ng/mL NGF.

## 2.7 Immunostaining of DRG

After culturing for 6 days, the DRG were immunostained with anti-neurofilament 200. Briefly, the samples were fixed in 3.7% formaldehyde at room temperature for 45 min, blocked with PBS containing 3% BSA for 1 h, and then incubated with the primary antibody anti-neurofilament 200 overnight at 4 °C. The anti-neurofilament 200 marker was detected using Alexa Fluor 488 goat anti-mouse IgG (1:200) secondary antibody at room temperature for 1 h. Between each procedure, the samples were washed three times with PBS. After staining, fluorescence micrographs were captured using a laser confocal scanning microscope (Zeiss LSM 700). The average lengths of extending neurites on either side of the DRG mass were calculated from fluorescence images by choosing 10 neurites from each side and measuring their length in ImageJ. Statistical analysis was performed using Student's t-test by analysis of variance at a 95% confidence level.

## 3. Results and Discussion

### 3.1 Characterization of PCL Nanofibers

As documented in literature, exposure to O<sub>2</sub>-plasma introduces oxygen single-bonded to carbon (–C–OH or –C–O–) and carbonyl groups (–C=O) to the surface of PCL nanofibers, making the initially hydrophobic nanofibers hydrophilic.<sup>19,30,35,36</sup> The hydrophilicity is necessary not only for cell attachment and growth on nanofibers, but also for successful aqueous treatments and modifications.<sup>19,30</sup> Figure S1 shows SEM images of the nanofiber mats after being exposed to plasma for different durations of time. When compared to pristine PCL nanofibers, no discernable changes in nanofiber morphology was found after the nanofibers had been exposed to plasma for 0.5, 1, and 2 min. However, after 5 min of plasma exposure, the nanofibers began to melt and rupture. So all nanofiber samples used in the present work were exposed to plasma for 2 min from this point forward.

After plasma treatment, the PCL nanofiber sections were separately immersed in PBS, 0.1% BSA solution, and 0.5% BSA solution for 1 h. Figures 2, S2 and S3, show SEM images of the nanofiber samples at different magnifications. Compared to the pristine sample, the treated nanofibers exhibited no change in morphology or texture. However, plasma treatment and subsequent immersion in PBS caused the nanofibers to swell from an average diameter of 210±7 nm to 243±7 nm (Figure S4). The adsorption of BSA onto the nanofibers further increased the average diameter to 257±9 nm or 264±8 nm after the samples had been immersed in 0.1% and 0.5% BSA solutions, respectively. The difference in diameter between the BSA-soaked and PBS-soaked nanofibers (14 nm or 21 nm) is less than twice the size of the long axis of a BSA protein, which is often modeled as an ellipsoid with two short axes of 4 nm in length and a long axis of 14 nm in length.<sup>37</sup> According to previous literature, proteins tend to spread across a surface during adsorption and only adsorb in monolayers.<sup>38,39</sup> In the more-concentrated 0.5% BSA solution, the rate of adsorption was greater than that of the 0.1% solution and, therefore, the BSA proteins were packed tighter with less spreading, which would explain the discrepancy in diameters of the two BSA-



exposed samples.<sup>39</sup> To demonstrate the surface hydrophilicity of the nanofiber mats, we measured their water contact angles. From Figure S5, when compared to that of the pristine PCL nanofibers, the surface contact angle of the nanofiber mat after O<sub>2</sub>-plasma treatment for 2 min was decreased from 126° to 54°. For the nanofibers adsorbed with BSA, the water droplet immediately soaked into the nanofibers, indicating the great improvement in the hydrophilicity of the nanofiber mats.

### 3.2 BSA Adsorption Kinetics

The adsorption of proteins onto the surfaces of nanofibers depends on several physiochemical properties such as the surface energy, hydrophobicity, and ionic or electrostatic interaction strength between proteins and nanofibers.<sup>40</sup> Figure 3A shows the relative fluorescence intensities of the nanofibers as the function of soaking time in the 0.1% and 0.5% BSA solutions. The fluorescence intensity represents the amount of the BSA-FITC adsorbed on the electrospun nanofibers, in another word, the amount of space left by the adsorbed BSA. From the plot of the adsorption of BSA onto the nanofibers in a 0.1% BSA solution, the fluorescence intensity decreases with time, indicating that the amount of adsorbed BSA increases with time. The adsorption of BSA from a 0.5% solution shows that the rate of BSA adsorption increases with solution concentration. In addition, there is a point of saturation at which the adsorbed BSA occupies all of the available space on the nanofibers. Therefore, the adsorption of BSA on PCL nanofibers is a time- and concentration-dependent process.

To better represent the actual adsorption of BSA on the nanofibers for different exposure durations, we plotted the net difference in fluorescence intensity over time by subtracting the relative fluorescence intensity at each time point from the relative fluorescence intensity of the section that was only exposed to BSA-FITC. Figure S6A shows the net difference in fluorescence intensity as a function of time, reflecting the time- and concentration-dependent nature of BSA adsorption. The plot can be linearized by a Hanes-Woolf transform (Figure S6B), which is accomplished by calculating the time elapsed over the change in fluorescent intensity and plotting against the time elapsed. Saturation coverage,  $c_{\max}$ , and a time to achieve half of the saturation coverage,  $T_m$ , could then be extracted from the slope and intercept values of the fitted plots, respectively. For both the 0.1% and 0.5% BSA solutions, the  $c_{\max}$  values are similar, 1.15 and 0.97, respectively, indicating that both solutions can saturate the PCL nanofibers to the same degree. However, the  $T_m$  values are vastly different, 15.85 and 0.61 min, respectively, and support the observation that the rate of BSA adsorption is higher for the more concentrated 0.5% BSA solution. We chose to make gradients with the 0.1% BSA solution because the  $T_m$  is too short to make a gradient with the 0.5% BSA solution. At a 0.5% concentration, BSA would almost immediately adsorb onto the nanofibers and limit the area of bare regions on the nanofibers for the bioactive protein to adsorb.

### 3.3 Generation of BSA Gradient

Because the adsorption of BSA onto PCL nanofibers is time dependent, a gradient can be created along a length of nanofibers by varying the duration of time a BSA solution is in contact with the nanofibers (Figure 1). In this work, we controlled the extent of BSA

exposure by placing strips of nanofibers vertically in a beaker and filling the beaker up with 0.1% BSA solution at a constant rate. With this approach, the nanofibers at the bottom of the strip were exposed to the BSA solution for a longer period of time than those at the top, and as a result, more BSA adsorbed onto the bottom region. We used BSA-FITC to fill in the bare regions left behind by the plain BSA and to visualize how a bioactive protein gradient might appear. Figure 3B shows the representative fluorescence micrographs and the corresponding relative fluorescence intensities of the strips made of electrospun nanofiber mat at different positions along the strips. The BSA amount adsorbed on the strips increase across the length of the vertically oriented strip of nanofibers, indicating the generation of a BSA gradient. Since the gradients were developed over the course of 1 h in 0.1% BSA solution, it is no surprise the curve shape of the gradient on the nanofiber strips (Figure 3B) is similar to that of the adsorption time course (Figure 3A). Besides, the BSA gradient generated on three different strips under the same experimental conditions were proved to be similar, demonstrating the robustness of this gradient-generating strategy. When the strip with BSA-FITC gradient was further soaked in PBS for 7 days, the fluorescence intensity of the strip showed no obvious change, indicating that the gradient was stable for at least 7 days. This could be explained by the fact that proteins tend to spread across a surface during adsorption and only adsorb in monolayers, which would be bound irreversibly given enough time and space.<sup>38,39</sup> Protein that was only bound reversibly would be washed away when exposed to buffer solution. After each adsorption step (BSA, BSA-FITC, or NGF), we washed the fibers with pure PBS or Tween 20 solution to remove any protein not completely adsorbed to the nanofiber surface. Therefore, the resultant gradient was consisted of irreversibly bound protein and the gradient would remain intact as long as the scaffold remains the same.

To visualize the gradient of BSA, we also created a gradient of BSA-FITC along the length of the pristine nanofiber strip by varying the duration of time a 0.1% BSA-FITC solution was in contact with the nanofibers. Figure S7 shows the corresponding relative fluorescence intensities of the nanofiber strip at different positions. The fluorescence intensities on the strip increased across the length of the vertically oriented strip of nanofibers, indicating the generation of a BSA-FITC gradient. Therefore, we were able to generate a preliminary BSA masking gradient on the PCL nanofibers, after which different kinds of bioactive proteins could be adsorbed on the free sites on the nanofibers to generate a countercurrent gradient. Next, we used NGF as a model growth factor to demonstrate the influence of a growth factor gradient would have on DRG neurite extension.

### 3.4 Extension of DRG Neurites

Peripheral nerve injuries often require grafts to reconnect the proximal and distal ends of a severed nerve and restore function. To avoid the usual pitfalls associated with auto- or allografts, research is focusing on developing tissue-engineering scaffolds that incorporate the most important aspects of innate nerve fiber conduits. The organization of ECM within the lumen of a nerve conduit is aligned longitudinally to direct nerve axons and glial cells from the spinal cord to their target while also providing shielding from the stresses of repeated stretching and contracting during movement. To this end, much research has been conducted on the behavior of DRG on aligned nanofiber scaffolds and found that aligned



nanofibers are essential to guide and direct neurite extension.<sup>16,41</sup> We attempted to further encourage neurite extension by generating an NGF gradient along the same direction as the aligned nanofibers. Figure S8 shows the high-degree of alignment of the nanofibers as revealed by SEM. With the same procedure as described above, BSA was adsorbed to the aligned nanofibers as a masking gradient, and NGF was then deposited on the BSA-blocked nanofibers to create an NGF gradient.

Chick DRG cells were seeded on the aligned PCL nanofibers functionalized with either a homogeneous or gradient distribution of NGF and cultured for 6 days. Figure 4 shows fluorescence micrographs of the stained neurites extending from the DRG cell mass. The average neurite length extending from each side of the DRG mass was evaluated from the images and is displayed in Figure 5. As a control, we also seeded DRG on the BSA-blocked aligned PCL nanofibers. Figure S9 shows the fluorescence micrographs of the neurites extending from DRG on the BSA-blocked nanofibers and the respective average neurite length. In all cases, neurites projected out from the DRG cell mass following the alignment of the PCL nanofibers because of the contact guidance provided by the underneath nanofibers, which corroborates previous results.<sup>42</sup> The presence of free NGF in the cell medium slightly increased the average neurite length regardless of the nature of the adsorbed protein. When NGF or BSA was adsorbed homogeneously on the nanofibers, neurites extended equally on either side of the DRG cell mass. On the other hand, when a gradient of NGF was generated on the nanofibers, increasing from left to right as directed by the arrow in Figure 4, the neurites on the right side of the DRG cell mass extended significantly farther than those on the left side, which was almost 40% longer. Growing on the nanofibers with NGF adsorbed, the growth cone of the DRG neurite recognizes the growth factor, expands its membrane, and then reaches for the next bound factor.<sup>42</sup> The adsorbed NGF increases the adherence of growth cones to the substrate, which promotes neurite extension by providing an anchor to further expand the growth cone. By increasing the NGF concentration along the nanofibers, the cell neurite growth cone could sense more growth factor within its reach and thus further expand its membrane along the direction of the gradient.<sup>43</sup> Therefore, on the scaffolds with an NGF gradient, the neurites extending towards the increasing NGF concentration were significantly longer than neurites extending against the gradient. Besides, the DRG cells cultured on NGF-adsorbed nanofibers (Figure 4) had thickened neurites compared with those cultured on BSA-adsorbed nanofibers (Figure S9).

## Conclusion

We have demonstrated a general strategy for generating gradients of bioactive proteins on electrospun nanofiber mats by masking with BSA. The adsorption of BSA onto nanofibers is a time- and concentration-dependent process. By linearly increasing the volume of BSA solution introduced into a container with a vertically oriented strip of nanofibers stood up in, a gradient in BSA is generated across the length of the nanofiber strip. The vacancies left by the BSA gradient are then filled with a bioactive protein of interest to produce a countercurrent gradient. This technique is simple and general, and it can be used to reduce the usage of expensive growth factor in generating a gradient and can also be easily adapted to various types of growth factors and nanofiber polymer systems. As a demonstration, a gradient of NGF is created on aligned PCL nanofibers along the direction of orientation. The

neurites extending along the gradient (*i.e.*, increase of NGF concentration) are significantly longer than those extending against the gradient. With this initial success, future studies can be conducted with various combinations of the bioactive proteins, cell types, and nanofiber architectures for specific applications related to regulating cell migration and improving tissue regeneration.

## Supplementary Material

Refer to Web version on PubMed Central for supplementary material.

## Acknowledgments

This work was supported by a grant from the NIH (R01 EB020050) and startup funds from the Georgia Institute of Technology.

## References

1. Tucker K, Meyer M, Barde Y. *Nat Neurosci.* 2001; 4:29–37. [PubMed: 11135642]
2. Gundersen R, Barrett J. *Science.* 1979; 206:1079–1080. [PubMed: 493992]
3. Junger W. *Nat Rev Immunol.* 2011; 11:201–212. [PubMed: 21331080]
4. Iijima M, Devreotes P. *Cell.* 2002; 109:599–610. [PubMed: 12062103]
5. Liu L, Ratner B, Sage E, Jiang S. *Langmuir.* 2007; 23:11168–11173. [PubMed: 17892312]
6. Gunawan R, Silvestre J, Gaskins H, Kenis P, Leckband D. *Langmuir.* 2006; 22:4250–4258. [PubMed: 16618172]
7. Arnold M, Hirschfeld-Warneken V, Lohmüller T, Heil P, Blümmel J, Cavalcanti-Adam E, López-García M, Walther P, Kessler H, Geiger B, Spatz J. *Nano Lett.* 2008; 8:2063–2069. [PubMed: 18558788]
8. Dertinger S, Jiang X, Li Z, Murthy V, Whitesides G. *Proc Natl Acad Sci U S A.* 2002; 99:12542–12547. [PubMed: 12237407]
9. Chung B, Flanagan L, Rhee S, Schwartz P, Lee A, Monuki E, Jeon N. *Lab Chip.* 2005; 5:401–406. [PubMed: 15791337]
10. Millet L, Stewart M, Nuzzo R, Gillette M. *Lab Chip.* 2010; 10:1525–1535. [PubMed: 20390196]
11. Wang Y, Irvine D. *Biomaterials.* 2011; 32:4903–4913. [PubMed: 21463892]
12. Zhao X, Jain S, Larman H, Gonzalez S, Irvine D. *Biomaterials.* 2005; 26:5048–5063. [PubMed: 15769541]
13. DeLong S, Moon J, West J. *Biomaterials.* 2005; 26:3227–3234. [PubMed: 15603817]
14. Xie J, Li X, Lipner J, Manning C, Schwartz A, Thomopoulos S, Xia Y. *Nanoscale.* 2010; 2:923–926. [PubMed: 20648290]
15. Gillies A, Bushong E, Deerinck T, Ellisman M, Lieber R. *Microsc Microanal.* 2014; 20:1835–1840. [PubMed: 25275291]
16. Xie J, MacEwan M, Li X, Sakiyama-Elbert S, Xia Y. *ACS Nano.* 2009; 3:1151–1159. [PubMed: 19397333]
17. Wagenseil J, Mecham R. *Physiol Rev.* 2009; 89:957–989. [PubMed: 19584318]
18. Liu W, Thomopoulos S, Xia Y. *Adv Healthcare Mater.* 2012; 1:10–25.
19. Yoo H, Kim T, Park T. *Adv Drug Delivery Rev.* 2009; 61:1033–1042.
20. Jordan A, Viswanath V, Kim S, Pokorski J, Korley L. *J Mater Chem B.* 2016; 4:5958–5974.
21. Zheng W, Wang Z, Song L, Zhao Q, Zhang J, Li D, Wang S, Han J, Zheng X, Yang Z, Kong D. *Biomaterials.* 2012; 33:2880–2891. [PubMed: 22244694]
22. Kim T, Park T. *Tissue Engineering.* 2006; 12:221–233. [PubMed: 16548681]
23. Choi J, Leong K, Yoo H. *Biomaterials.* 2008; 29:587–596. [PubMed: 17997153]
24. Rieger K, Birch N, Schiffman J. *J Mater Chem B.* 2013; 1:4531–4541.

25. Ji W, Sun Y, Yang F, van den Beucken J, Fan M, Chen Z, Jansen J. *Pharm Res.* 2011; 28:1259–1272. [PubMed: 21088985]
26. Kim J, Im B, Jin G, Jang J. *ACS Appl Mater Interfaces.* 2016; 8:22721–22731. [PubMed: 27513165]
27. Viswanathan P, Themistou E, Ngamkham K, Reilly G, Armes S, Battaglia G. *Biomacromolecules.* 2015; 16:66–75. [PubMed: 25402847]
28. Dinis T, Elia R, Vidal G, Auffret A, Kaplan D, Egles C. *ACS Appl Mater Interfaces.* 2014; 6:16817–16826. [PubMed: 25203247]
29. Kim S, Wallat J, Harker E, Advincula A, Pokorski J. *Polym Chem.* 2015; 6:5683–5692. [PubMed: 26604990]
30. Shi J, Wang L, Zhang F, Li H, Lei L, Liu L, Chen Y. *ACS Appl Mater Interfaces.* 2010; 2:1025–1030. [PubMed: 20423122]
31. Li X, Xie J, Lipner J, Yuan X, Thomopoulos S, Xia Y. *Nano Lett.* 2009; 9:2763–2768. [PubMed: 19537737]
32. Liu W, Zhang Y, Thomopoulos S, Xia Y. *Angew Chem Int Edit.* 2013; 52:429–432.
33. Liu W, Lipner J, Xie J, Manning C, Thomopoulos S, Xia Y. *ACS Appl Mater Interfaces.* 2014; 6:2842–2849. [PubMed: 24433042]
34. Bowers D, Tanes M, Das A, Lin Y, Keane N, Neal R, Ogle M, Brayman K, Fraser C, Botchwey E. *ACS Nano.* 2014; 8:12080–12091. [PubMed: 25426706]
35. Martins A, Pinho E, Faria S, Pashkuleva I, Marques A, Reis R, Neves N. *Small.* 2009; 5:1195–1206. [PubMed: 19242938]
36. Pappa A, Karagkiozaki V, Krol S, Kassavetis S, Konstantinou D, Pitsalidis C, Tzounis L, Pliatsikas N, Logothetidis S. *Beilstein J Nanotechnol.* 2015; 6:254–262. [PubMed: 25671169]
37. Wright A, Thompson M. *Biophys J.* 1975; 15:137–141. [PubMed: 1167468]
38. Latour R. *Encycl Biomater Biomed Eng.* 2005:1–15.
39. Kim J, Somorjai G. *J Am Chem Soc.* 2003; 125:3150–3158. [PubMed: 12617683]
40. Jiang T, Carbone E, Lo K, Laurencin C. *Prog Polym Sci.* 2015; 46:1–24.
41. Xie J, Liu W, MacEwan M, Bridgman P, Xia Y. *ACS Nano.* 2014; 8:1878–1885. [PubMed: 24444076]
42. Kapur T, Shoichet M. *J Biomed Mater Res A.* 2004; 68:235–243. [PubMed: 14704965]
43. Cao X, Shoichet M. *Neuroscience.* 2001; 103:831–840. [PubMed: 11274797]

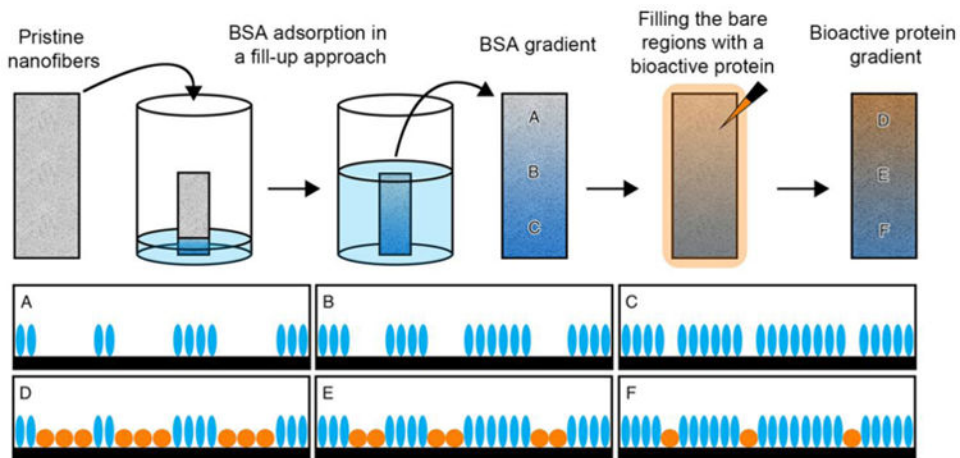


**Figure 1.**

A schematic of the procedure used for generating a gradient of bioactive protein on a nanofiber scaffold. A mat of plasma-treated nanofibers, which has been mounted on a glass slide, is vertically placed in a beaker while a BSA solution is slowly added to create a gradient of inert protein such as BSA (A-C). The bare regions left behind are then filled with a bioactive protein (*e.g.*, a growth factor or adhesive protein) to produce a gradient that runs countercurrent to the BSA gradient (D-F).

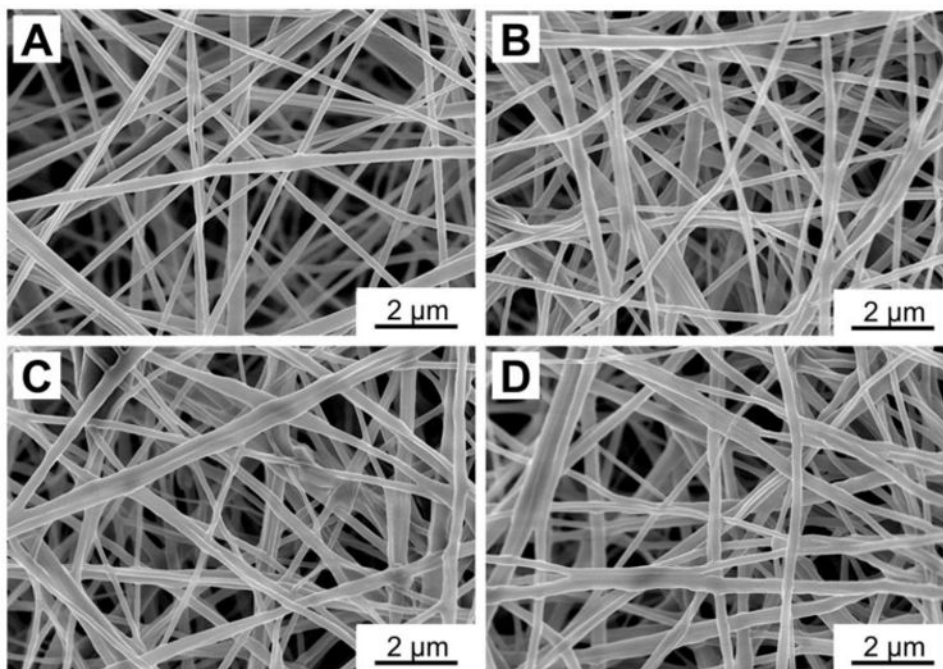


**Figure 2.** SEM images of random PCL nanofibers (A) before and (B–D) after plasma treatment for 2 min, followed by soaking in (B) PBS, (C) 0.1% BSA solution, and (D) 0.5% BSA solution, respectively, for 1 h. The morphology and texture of the nanofibers are essentially preserved during the treatments.

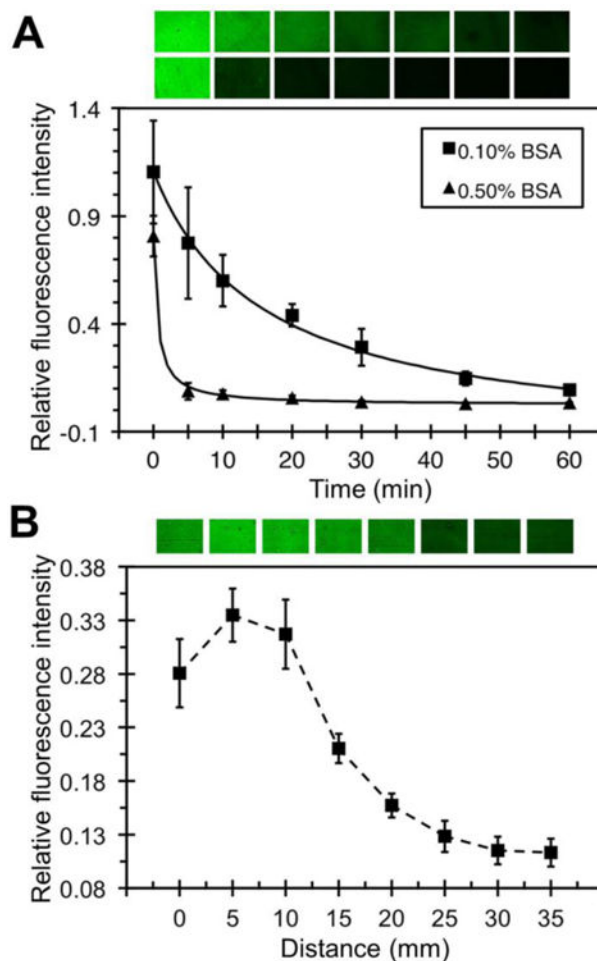


**Figure 3.**

(A) Plots of the relative fluorescence intensities for the BSA-FITC adsorbed on the nanofibers as a function of soaking time in the 0.1% and 0.5% BSA solutions, respectively. The corresponding representative fluorescence micrographs of the nanofibers are also included (upper row: 0.1% BSA, and lower row: 0.5%). The extent of BSA adsorbed on PCL nanofibers is dependent on the duration of exposure to BSA solution ( $n=3$  for each time point). The BSA concentration also affects the rate at which BSA adsorbs onto the nanofibers. (B) Representative fluorescence micrographs and their corresponding relative fluorescence intensities at different positions of nanofiber strips by varying the duration of contact time with a 0.1% BSA solution over a distance of 35 mm ( $n=9$  at each position). A gradient in BSA can be clearly seen across the strip of nanofibers.



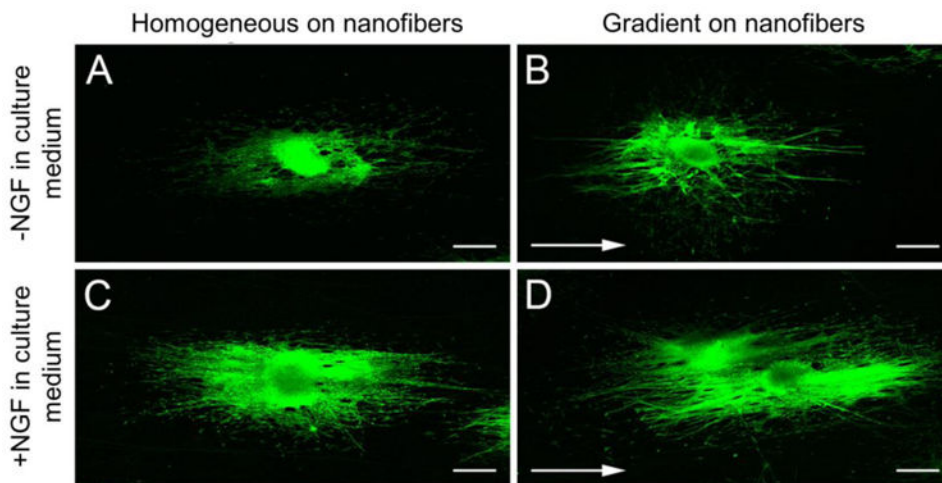


**Figure 4.** Fluorescence micrographs showing the neurites extending from DRG when cultured on aligned PCL nanofibers with NGF adsorbed on the surface in a (A, C) homogeneous form and (B, D) gradient, respectively, while in the (A, B) absence or (C, D) presence of free NGF in the culture media. The neurites were stained with anti-neurofilament 200 (green). The white arrows indicate the direction of NGF gradient increase. Scale bar: 500  $\mu\text{m}$ .

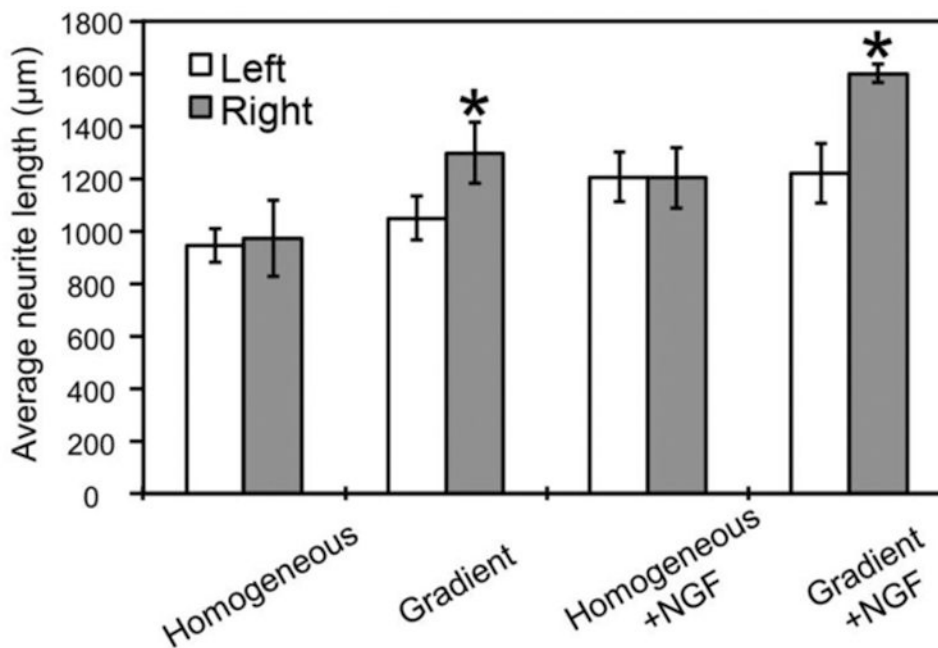


**Figure 5.**

The average lengths of the neurites extending from the left side (decreasing of NGF concentration) and right side (increasing of NGF concentration) of the DRG mass when cultured on the aligned PCL nanofibers with NGF adsorbed on the surface in a homogeneous and gradient profile, respectively, in the absence or presence (+NGF) of free NGF in the culture media. \* $P < 0.05$  when compared to the left side of the DRG mass.